Long-Lived Radical Cations as Model Compounds for the Reactive One-Electron Oxidation Product of Vitamin E

Hong Mei Peng,[†] Becky F. Choules,[†,§] Wei Wei Yao,[†] Zhengyang Zhang,[†] Richard D. Webster,*[,†] and Peter M. W. Gill[‡]

Division of Chemistry and Biological Chemistry, School of Physical and Mathematical Sciences, Nanyang Technological University, Singapore 637371, and Research School of Chemistry, Australian National University, Canberra ACT 0200, Australia

Received: May 10, 2008; Revised Manuscript Received: June 9, 2008

Heterocyclic compounds with structures similar to vitamin E, but without the hydroxyl hydrogen atom, were synthesized and their electrochemical behavior examined in acetonitrile solutions and as solids in aqueous solutions of varying pH by attaching the compounds to the surface of a glassy carbon electrode. Compound **1**, containing a fully methylated aromatic ring was found to be the most long-lived following one-electron oxidation, with its radical cation ($\mathbf{1}^{+\bullet}$) surviving in acidic aqueous solutions and able to be isolated as a salt, $\mathbf{1}^{+\bullet}(SbF_6^-)$, when reacted with $NOSbF_6$ in CH_3CN. Electrochemical, UV−vis and FTIR experiments on $\mathbf{1}^{+\bullet}$, in addition to the results from theoretical calculations, indicated that the electrochemical, electronic and structural properties of $\mathbf{1}^{+\bullet}$ are very similar to those of the radical cation of vitamin E.

1. Introduction

There are currently two conflicting views on the role of vitamin E in mammalian biological systems. One theory is that vitamin E acts solely as an antioxidant (essentially a sacrificial compound) in order to inhibit lipid peroxidation via a well-established free radical terminating mechanism.[1] The second hypothesis is that vitamin E has a specific role as a cellular signaling molecule, although the exact mechanism is not currently understood.[2] It is likely that the latter mechanism, should it occur, involves oxidized forms of vitamin E in addition to the phenolic starting material. Therefore, detailed understanding of the oxidative behavior of vitamin E could lead to a better understanding of potential in vivo biological reactions of vitamin E.

Vitamin E can be electrochemically oxidized in a series of electron-transfer and proton transfer reactions that have interesting similarities and differences to those commonly encountered during the oxidation of other phenolic compounds.[3] In acetonitrile or dichloromethane solutions in the absence of added acid or base, α-tocopherol (α-TOH) (the fully methylated form of vitamin E) undergoes two one-electron transfers and one-proton loss to form the phenoxonium cation (α-TO^+) (Scheme 1a).[4,5] The reaction occurs via two one-electron steps because the phenoxyl radical (α-$TO^\bullet$) formed by loss of the proton from the radical cation, α-$TOH^{+\bullet}$, is easier to oxidize than the starting material by ~ -1.5 V,[5a,6] so is thus immediately further oxidized to α-TO^+.[4,5b] The importance of the radical cation in the biological chemistry of vitamin E is presently unknown,[1d] although it is potentially an interesting intermediate compound because it is relatively nonacidic (in nonaqueous media) compared to most other phenolic radical cations.[3d] The phenoxonium cation is surprisingly long-lived and can even be isolated from solution and the X-ray structure determined.[5e] The electrochemical reactions in Scheme 1a are completely chemically reversible, so that applying a sufficiently negative potential leads to the quantitative regeneration of the starting material.[5] The reason for the chemical reversibility is that the equilibrium constant for the proton transfer reaction is ≪1, and the rate

SCHEME 1: (*a*) Oxidation Mechanism (ECE) for α-Tocopherol in CH_3CN, Consisting of Two One-Electron Steps and One-Proton Transfer; (*b*) Corresponding One-Electron Oxidation Mechanism (E) for Compound 1; (*c*) 6-Chromanol; (d) Isomeric Forms of Compounds 2 (2a/2b) and 3 (3a/3b)

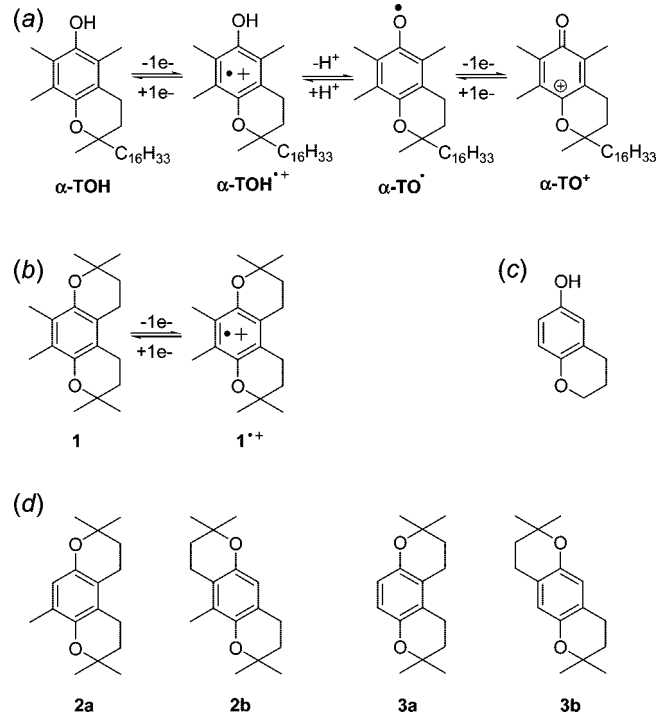

* To whom correspondence should be addressed. E-mail: webster@ntu.edu.sg.
† Nanyang Technological University.
‡ Australian National University.
§ Present Address: School of Chemistry, University of Edinburgh, King's Buildings, West Mains Road, Edinburgh, UK EH9 3JJ.

10.1021/jp804135e CCC: $40.75
Published on Web 07/29/2008

constant for the protonation reaction is extremely fast (close to diffusion controlled).[5h]

In this work, we were interested in examining the importance of the phenolic structure on the one-electron oxidation of vitamin E, by examining the electrochemical behavior of compounds **1**−**3** [Scheme 1] that were synthesized without the phenolic hydrogen atom but still maintaining the heterocyclic ring from 6-chromanol (Scheme 1c). Compound **1** (Scheme 1b) was obtained as one isomer while compound **2** contains a mixture of the two isomers, **2a** and **2b**, and compound **3** contains a mixture of **3a** and **3b** (Scheme 1d). The isomers were not separated; therefore, the experimental results were obtained from mixtures of **2a/2b** and **3a/3c**. It was envisaged that the replacement of the hydrogen atom in vitamin E with a symmetrical ether linkage in compounds **1**−**3** would change the electrochemical response from a two-electron oxidation to a one-electron process, providing that the formed radical cations were long-lived (Scheme 1b). It was also of interest to determine the difference in potentials between the protic phenolic structure of vitamin E and the aprotic ring closed analogues (**1**−**3**).

2. Experimental Section

2.1. Chemicals. HPLC grade CH_3CN (Tedia) was used as received, and Bu_4NPF_6 was prepared and purified by standard methods.[7] Water with a resistivity of no less than 18 MΩ cm was used for experiments at different pH-values. Sulfuric acid was used for experiments at pH 1. Citric acid-phosphate buffer solutions (pH 3, 5, and 7) were prepared from disodium hydrogen phosphate (Merck) and citric acid (Amresco). Britton−Robinson buffer solutions (pH 9, 11, and 13) were prepared using 0.04 M acetic, phosphoric, and boric acids (Merck), and adjusted to the required pH using NaOH (Merck).

2.2. Synthetic Experiments. The synthesis of compounds **1**−**3** was based on a modified version of literature reports.[8]

Compound 1. 2,3-Dimethylbenzene-1,4-diol (276 mg, 2.0 mmol) and TsOH (38 mg, 0.2 mmol) were placed in a flask, and dry toluene (5 mL) was added under argon. 2-Methyl-but-3-en-2-ol (189 mg, 4.1 mmol) was injected dropwise into the flask by syringe, and the mixture was stirred for 18 h at 100 °C. After cooling, ethyl acetate was added to dilute the solution, and the organic layer was washed with water and brine and dried with Na_2SO_4. After the solvent was removed, the residue was separated by column chromatography to give a white solid (482 mg, 88%). ^{1}H NMR ($CDCl_3$, 300 MHz) δ: 2.55 (t, 4H, J = 13.6 and 6.8 Hz), 2.10 (s, 6H), 1.78 (t, 4H, J = 13.7 and 6.8 Hz), 1.29 (s, 12H). ^{13}C {^{1}H} NMR ($CDCl_3$, 75 MHz) δ: 144.7, 123.4, 115.5, 72.4, 33.0, 26.9, 20.1, 11.8.

Compound 2 (Obtained As Two Isomers, 2a and 2b). 2-Methylbenzene-1,4-diol (248 mg, 2.0 mmol) and TsOH (38 mg, 0.2 mmol) were placed in a flask, and dry toluene (5 mL) was added under argon. 2-Methyl-but-3-en-2-ol (206 mg, 2.4 mmol) was injected dropwise into the flask by syringe, and the mixture was stirred for 18 h at 100 °C. The same procedure as used for **1** was used to work up this reaction, and the product was obtained as a white solid (143 mg, 46%).

Compound 3 (Obtained As Two Isomers, 3a and 3b). Hydroquinone (220 mg, 2.0 mmol) and TsOH (38 mg, 0.2 mmol) were placed in a flask, and dry toluene (5 mL) was added under argon. 2-Methyl-but-3-en-2-ol (189 mg, 2.2 mmol) was injected dropwise into the flask by syringe, and the mixture was stirred for 18 h at 80 °C. The same procedure as used for **1** was used to work up this reaction, and the product was obtained as a white solid (135 mg, 50%).

Chemical Oxidation of Compound 1. In a glovebox, to a solution of **1** in 1 mL acetonitrile was added $NOSbF_6$ (1 equiv) in one pot, and the solution became black immediately. After the mixture was stirred for ten minutes, the solvent was removed to give a dark yellow solid [$\mathbf{1}^{+\bullet}$ (SbF_6^-)], which was analyzed by infrared spectroscopy, UV−vis spectroscopy, and elemental analysis. Anal. calcd for $C_{18}H_{26}F_6O_2Sb$ (510.15): C, 42.38; H, 5.14. Found: C, 42.71; H, 4.94.

SCHEME 2: Cross-Coupling Products Obtained via the Oxidation of 2a/2b and 3a/3b with One mol Equivalent of $NOSbF_6$ in CH_3CN

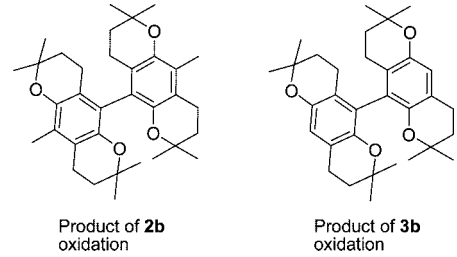

Chemical Oxidation of Compound 2. In a glovebox, to a solution of **2a/2b** in 1 mL acetonitrile was added $NOSbF_6$ (1 equiv) in one pot, and the solution became black immediately. After the mixture was stirred for ten minutes, the solution was removed from the glovebox and stirred in air for 12 h. After the solvent was removed, the residue was chromatographed on silica gel with hexane/ethyl acetate = 10:1 to give the cross-coupled product as a yellow solid (24%) (Scheme 2). ^{1}H NMR ($CDCl_3$, 400 MHz) δ: 2.56 (t, 4H, J = 13.6 and 6.8 Hz), 2.06 (s, 3H, Ar-CH_3), 1.86−1.79 (m, 4H), 1.29 (s, 12H). ^{13}C {^{1}H} NMR ($CDCl_3$, 100 MHz) δ: 144.6, 140.9, 137.8, 121.0, 118.3, 116.9, 74.4, 73.5, 32.32, 32.29, 26.64, 26.27, 20.24, 19.81, 10.4 (Ar-CH_3). HRMS (ESI) calcd for $C_{34}H_{47}O_4$: 519.3474. Found: 519.3456.

Chemical Oxidation of Compound 3. In a glovebox, to a solution of **3a/3b** in 1 mL acetonitrile was added $NOSbF_6$ (1 equiv) in one pot, and the solution became black immediately. After the mixture was stirred for ten minutes, the solution was removed from the glovebox and stirred in air for 12 h. After the solvent was removed, the residue was chromatographed on silica gel with hexane/ethyl acetate = 10:1 to give the cross-coupled product as a yellow solid (20%) (Scheme 2). ^{1}H NMR ($CDCl_3$, 400 MHz) δ: 6.63 (s, 1H, Ar-CH), 2.73 (t, 2H, J = 13.6 and 6.8 Hz), 2.65 (t, 2H, J = 13.2 and 6.8 Hz), 1.81 (t, 2H, J = 13.2 and 6.4 Hz), 1.76 (t, 2H, J = 13.6 and 6.4 Hz), 1.31 (s, 12H). ^{13}C {^{1}H} NMR ($CDCl_3$, 100 MHz) δ: 146.2, 140.3, 139.2, 122.3, 119.0, 112.2, 75.5, 74.1, 32.4, 31.7, 26.5, 22.2, 18.2. HRMS (ESI) calcd for $C_{32}H_{43}O_4$: 491.3161. Found: 491.3138.

^{1}H and ^{13}C NMR spectra of compounds **2a/2b** and **3a/3b** and the products obtained from chemical oxidation experiments using $NOSbF_6$ in CH_3CN are provided in the Supporting Information section.

2.3. Electrochemical Measurements. Cyclic voltammetry (CV) experiments were conducted with a computer controlled Eco Chemie Autolab PGSTAT 100 with an ADC fast scan generator. Working electrodes were 1 mm or 5 mm diameter planar Au, Pt, or glassy carbon (GC) disks, used in conjunction with a Pt auxiliary electrode. For nonaqueous experiments, a Ag wire reference electrode was connected to the test solution via a salt bridge containing 0.5 M Bu_4NPF_6 in CH_3CN with accurate potentials obtained by using ferrocene (Fc) as an internal standard. An Ag/AgCl reference electrode containing 3 M KCl was used for experiments in aqueous systems.

Bulk oxidation experiments were performed in a divided controlled potential electrolysis (CPE) cell separated with a

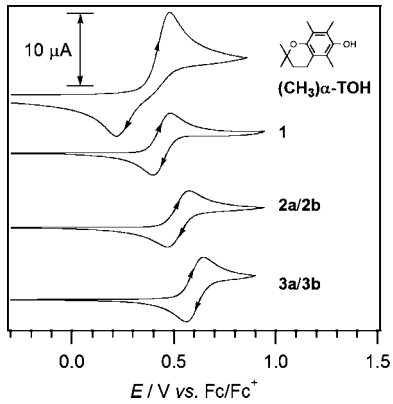

Figure 1. Cyclic voltammograms of 2.0 mM compounds in CH_3CN with 0.2 M n-Bu_4NPF_6 recorded at a 1 mm diameter Pt electrode at T = 293 K. Oxidative current increases in the upward direction.

porosity number 5 (1.0−1.7 μm) sintered glass frit.[9] The working and auxiliary electrodes were identically sized Pt mesh plates symmetrically arranged with respect to each other with an Ag wire reference electrode (isolated by a salt bridge) positioned to within 2 mm of the surface of the working electrode. The volumes of both the working and auxiliary electrode compartments were approximately 10 mL each. The solution in the working electrode compartment was simultaneously deoxygenated and stirred using bubbles of argon gas. The number of electrons transferred during the bulk oxidation process was calculated from

$$N = Q/nF \quad (1)$$

where N = number of moles of starting compound, Q = charge (coulombs), n = number of electrons, and F is the Faraday constant (96485 C mol^{-1}).

2.4. UV−vis-NIR and FTIR Measurements. In situ UV−vis spectra were obtained with a PerkinElmer Lambda 750 spectrophotometer in an optically semitransparent thin layer electrochemical (OSTLE) cell (path length = 0.05 cm) using a Pt mesh working electrode.[10] FTIR experiments were conducted with a Thermo Electron Nicolet 6700 spectrometer mainframe with a Continuμm infrared microscope.

2.5. Computational Procedures. Molecular orbital calculations were performed using a development version of the Q-Chem 3.1 software package[11] and the Spartan ′04 software package.[12] Harmonic vibrational frequencies were calculated by Q-Chem using the EDF2/6−31+G* density functional model[13] and the SG-1 quadrature grid,[14] and no empirical scale factors were applied.

3. Results

3.1. Cyclic Voltammetry. Figure 1 shows cyclic voltammograms of compounds **1**−**3** recorded at a scan rate of 100 mV s^{-1} in CH_3CN solutions, along with the α-tocopherol model compound, (CH$_3$)α-TOH, where the phytyl tail is replaced with a methyl group. The voltammograms in Figure 1 show that the anodic (i_p^{ox}) and cathodic (i_p^{red}) peak currents for (CH$_3$)α-TOH are larger than those observed for compounds **1**−**3**, at equivalent concentrations and scan rates. The larger i_p^{ox} value observed for (CH$_3$)α-TOH is due to the transfer of a greater number of electrons with the oxidation occurring by two electrons (two one-electron steps) and a proton loss to form the phenoxonium cation (α-TO$^+$) (Scheme 1a).[4,5] Compounds **1**−**3** with the aprotic cyclic ether in place of the protic phenol are unable to lose a hydroxyl proton (Scheme 1b); therefore they undergo a one-electron oxidation, with no follow-up chemical reaction apparent on the time-scale of the CV experiment.

The anodic (E_p^{ox}) to cathodic (E_p^{red}) peak separation (ΔE_{pp}) is much larger for (CH$_3$)α-TOH ($\Delta E_{pp} \approx 260$ mV) compared to compounds **1**−**3** ($\Delta E \approx 70$ mV) because of the presence of the proton transfer and multiple electron transfer steps (an ECE mechanism) for (CH$_3$)α-TOH. The $E^r_{1/2}$ values [$E^r_{1/2} = (E_p^{ox} + E_p^{red})/2$] for compounds **1**−**3** were calculated to be +0.440, +0.520, and +0.605 V versus Fc/Fc$^+$, respectively, (reported to the nearest 5 mV). The $E^r_{1/2}$ values for compounds **1**−**3** are a good approximation to the formal potentials (E^0_f) because the oxidation mechanism involves a simple chemically reversible one-electron transfer. For (CH$_3$)α-TOH, the $E^r_{1/2}$-value is not a good approximation for the formal one-electron oxidation potential because of the additional electron and proton transfer steps. Instead the formal one-electron oxidation potential for (CH$_3$)α-TOH in CH_3CN with Bu_4NPF_6 as the supporting electrolyte was previously estimated by digital simulation techniques[15] to be +0.50 ± 0.05 V versus Fc/Fc$^+$ at 293 K.[5h] It would be expected that **1**, rather than **2a/2b** or **3a/3b** should be closest in potential to (CH$_3$)α-TOH, because it is most closely related in structure (containing a fully methylated aromatic ring). Therefore, the $E^r_{1/2}$ of **1** obtained by voltammetric simulations may be closer to the lower estimated potential (+0.45 V versus Fc/Fc$^+$).[5h]

It can be concluded that the formal one-electron oxidation potential of α-TOH is very close (within 0.1 V) of that observed for compounds **1**−**3**, and therefore that the presence of the phenolic group does not strongly influence the formal one-electron oxidation potential of the chromanol. The $E^r_{1/2}$ values for compounds **1**−**3** shift to more negative potentials with increasing methylation of the aromatic ring. The shift in potential can be accounted for by the electron donating ability of the methyl groups, which provides further evidence that the molecular orbital involved in the one-electron oxidation is located within the aromatic and heterocyclic portions of the molecule. The observation of only one oxidation process for **2a/2b** (**2**) and **3a/3b** (**3**) indicates that the E^0_f values for the isomers are very close to each other. Digital simulation experiments indicate that one-electron processes that are electrochemically and chemically reversible on the CV time scale are indistinguishable if they are within approximately 30 mV of each other.[15]

3.2. Controlled Potential Electrolysis (CPE). In order to gain information about the lifetime of the radical compounds over longer timescales and to confirm the number of electrons transferred in the oxidation process, CPE and coulometry were conducted on compounds **1**−**3**. Figure 2a shows CV data obtained before (black line) and after (red line) the exhaustive electrolysis of **1**. Figure 2b,c shows the corresponding current/coulometry versus time data obtained during the oxidation of **1** and reduction of **1**$^{+\bullet}$, respectively. The data in Figure 2 illustrate that **1** is oxidized quantitatively in a one electron process to **1**$^{+\bullet}$ and that **1**$^{+\bullet}$ can be quantitatively reduced back to **1**. It was found that **1**$^{+\bullet}$ is very long-lived in CH_3CN solution, surviving for at least several weeks, and can be isolated as a solid compound via chemical oxidation with the one-electron oxidant $NO^+(SbF_6^-)$.

In contrast to **1**$^{+\bullet}$, compounds **2**$^{+\bullet}$ and **3**$^{+\bullet}$ survived for a shorter time under electrolysis conditions and a greater number of electrons were transferred ($n \approx 1.5$ electrons per molecule). Figure 3 shows CV data obtained before (black line) and after (red line) the exhaustive oxidation of **2**. In this case an additional reduction process is evident at the completion of the electrolysis

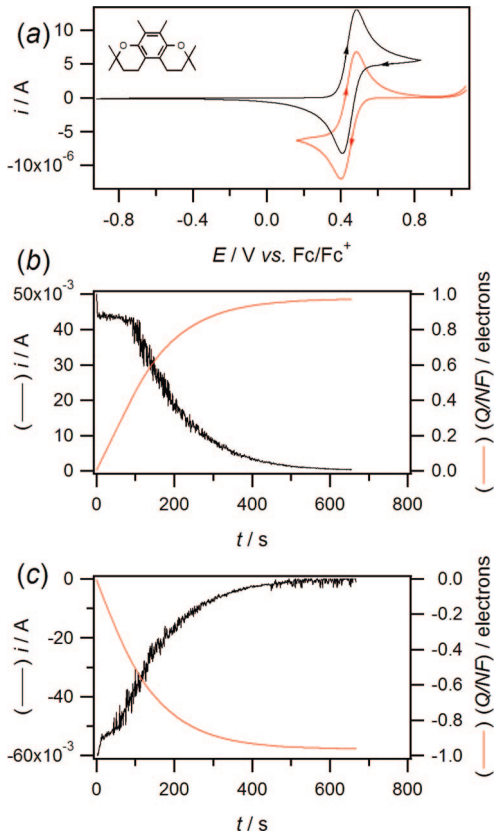

Figure 2. Voltammetric and coulometric data obtained at 293 K during the controlled potential electrolysis of 5 mM **1** in CH_3CN with 0.2 M Bu_4NPF_6. (a) Cyclic voltammograms recorded at a scan rate of 0.1 V s^{-1} with a 1.0 mm diameter Pt electrode. (Black line) Prior to the bulk oxidation of **1**. (Red line) After the exhaustive oxidation of **1**. (b) Current/coulometry versus time data obtained during the exhaustive oxidation of **1** at 0.6 V vs Fc/Fc^+. (c) Current/coulometry versus time data obtained during the reverse exhaustive reduction of $1^{+\bullet}$ at 0.2 V vs Fc/Fc^+.

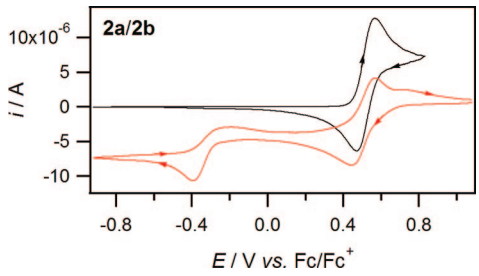

Figure 3. Cyclic voltammograms recorded at a scan rate of 0.1 V s^{-1} with a 1.0 mm diameter Pt electrode at 293 K during the controlled potential electrolysis of 5 mM **2** in CH_3CN with 0.2 M Bu_4NPF_6. (Black line) Prior to the bulk oxidation of **2**. (Red line) After the exhaustive oxidation of **2**.

at −0.4 V versus Fc/Fc^+, which is due to the formation of a reaction product of $2^{+\bullet}$. The process at −0.4 V remains when $2^{+\bullet}$ is reduced back to **2**. The CV data obtained during the electrolysis of **3** were very similar with an additional product detected at −0.4 V versus Fc/Fc^+ at the completion of the electrolysis. Both $2^{+\bullet}$ and $3^{+\bullet}$ with partial methyl substitution are able to undergo coupling reactions at the aromatic ring. Nevertheless, both $2^{+\bullet}$ and $3^{+\bullet}$ were able to be detected voltammetrically at the end of the electrolysis, indicating that their half-lives were several minutes in CH_3CN.

3.3. UV−vis Spectroscopy. In situ electrochemical UV−vis-NIR experiments were conducted in an optically semitransparent thin layer electrochemical cell on compounds **1**−**3**, with the spectra for $\mathbf{1}/\mathbf{1}^{+\bullet}$ given in Figure 4a. The starting material showed one band between 200−3300 nm at ∼300 nm, while the oxidized compound, $\mathbf{1}^{+\bullet}$, displayed a more intense absorbance at 313 nm and an additional band at 482 nm (with a shoulder at 456 nm). No absorbances were detected in the NIR region for **1** or $\mathbf{1}^{+\bullet}$. The thin-layer operation of the cell meant that exhaustive electrolysis occurred within 2 min; therefore, spectra were also obtained for $2^{+\bullet}$ and $3^{+\bullet}$ (without any appreciable signs of additional reaction products) that were very similar in appearance to $\mathbf{1}^{+\bullet}$.

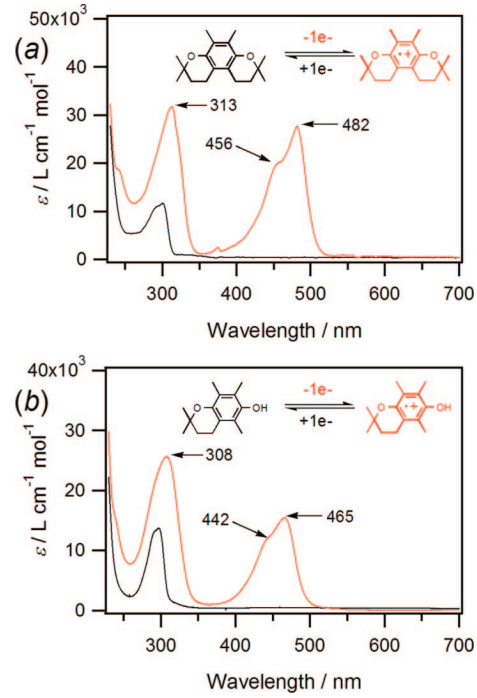

Figure 4. In situ electrochemical UV−vis spectra. (a) Obtained during the electrolysis of 0.2 mM **1** in CH_3CN at 293 K with 0.5 M Bu_4NPF_6. (Black line) **1**. (Red line) $\mathbf{1}^{+\bullet}$. (b) Obtained in CH_2Cl_2 containing 0.5 M Bu_4NPF_6 and 1 M CF_3COOH at 253 K during the sequential one-electron oxidation of 1 mM α-TOH. (Black line) α-TOH. (Red line) $\alpha\text{-TOH}^{+\bullet}$. Data in panel b were modified from reference.[5d]

Figure 4b shows the UV−vis spectrum of $[(CH_3)\alpha\text{-TOH}]^{+\bullet}$ that was obtained by oxidizing $[(CH_3)\alpha\text{-TOH}]$ in an organic solvent containing a very strong acid, thereby preventing the deprotonation of the phenol.[5d] The UV−vis spectrum of $[(CH_3)\alpha\text{-TOH}]^{+\bullet}$ is very similar to the spectrum of $\mathbf{1}^{+\bullet}$, which provides good evidence that the electronic transitions observed in the UV−vis spectrum of $[(CH_3)\alpha\text{-TOH}]^{+\bullet}$ are independent of the hydroxyl group and are associated with the aromatic and heterocyclic portions of the molecule. This is further supported by the ε-values for absorbances of the cation radicals, which are greater for $\mathbf{1}^{+\bullet}$ compared to $[(CH_3)\alpha\text{-TOH}]^{+\bullet}$, because $\mathbf{1}^{+\bullet}$ contains two heterocyclic rings (Figure 4).

3.4. Chemical Oxidation Experiments. Compounds **1**−**3** were reacted chemically with equivalent molar amounts of $NOSbF_6$ in CH_3CN at 20 ± 2 °C. The one-electron chemical oxidation of **1** produced $\mathbf{1}^{+\bullet}$ quantitatively that survived in solution for at least several weeks. Removal of the solvent under vacuum allowed the isolation of a solid sample of $\mathbf{1}^{+\bullet}$ (SbF_6^-) (the byproduct, NO•(g), is easily removed with the solvent).

In contrast to the simple oxidation of **1**, the one-electron oxidation of **2** and **3** led to the formation of a range of reaction products. Two products that were identified by NMR (^1H and ^{13}C) and high resolution mass spectrometry (HRMS) experi-

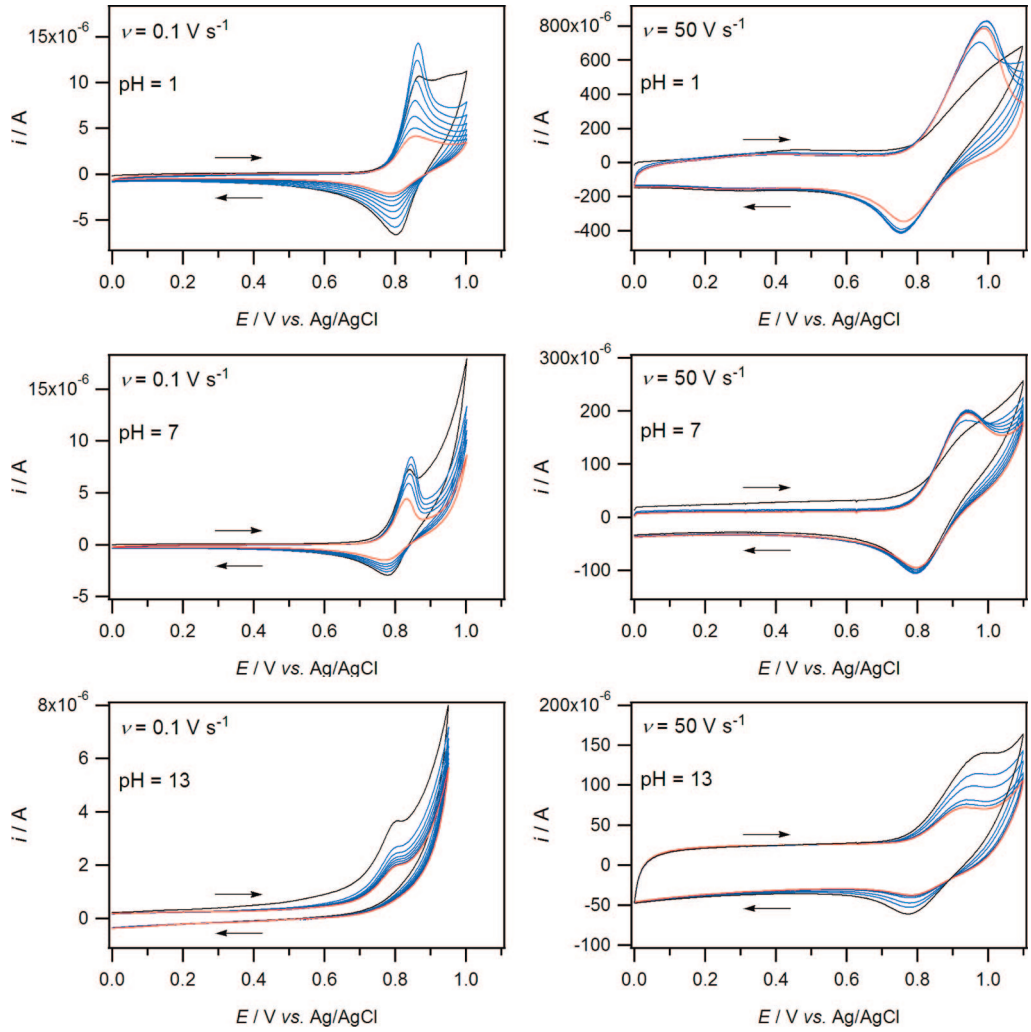

Figure 5. Multiple cycle solid state voltammograms of **1** recorded at two scan rates (ν) at a 5 mm diameter planar GC electrode at 25 °C. The surface of the electrode was prepared by allowing a 2 μL droplet from a 2 mM solution of **1** (in CH_3CN) to evaporate, then immersing the electrode in an aqueous solution at different pH-values. (Black line) First scan. (Blue lines) Sequential intermediate scans. (Red line) Final scan.

ments in 20−25% yield from the chemical oxidations of **2** and **3** were the cross-coupled products given in Scheme 2. The mechanism for the formation of the products can most simply be rationalized by dimerization of the cation radicals followed by the loss of two protons. An ECEC mechanism is also possible, where one cation radical reacts with the starting material to form a dimer cation radical, which subsequently undergoes further one-electron oxidation and proton loss processes. A range of other scenarios are possible depending on the order of the electron transfer and the homogeneous chemical steps. Thin-layer chromatography and NMR experiments indicated that a number of other products with complex spectra were also produced (which were not identified), which were likely to be the result of other cross-coupling reactions.

The chemical oxidation and electrolysis experiments indicate that $\mathbf{1}^{+\bullet}$ is long-lived in solution because of the steric hindrance introduced by its fully methylated aromatic ring preventing irreversible dimerization reactions, while $\mathbf{2}^{+\bullet}$ and $\mathbf{3}^{+\bullet}$ with fewer methyl groups have less steric hindrance at the aromatic ring and are able to undergo additional reactions.

3.5. Electrochemistry of Films Attached to GC Electrodes. Solid state electrochemical experiments were conducted by allowing a 2 μL droplet of a 2 mM solution of **1** in CH_3CN to evaporate from the surface of a 5 mm diameter GC electrode. The electrode was then immersed in an aqueous solution at different pH-values. Between 5−10 voltammetric cycles at a fixed scan rate and pH-value were recorded, before the electrode was rinsed with acetone, repolished, and then another droplet of the analyte deposited onto the surface and the procedure repeated at a different scan rate or pH-value. Similar experiments were conducted with Au and Pt electrodes, but the voltammograms showed only very small and poorly reproducible oxidation processes, so the discussion is limited to the GC surface.

Figure 5 shows representative voltammetric data obtained at two scan rates and three pH values for films of **1** on the electrode surface. At a scan rate of 0.1 V s^{-1}, a clear oxidation process was evident with an E_p^{ox} at ~+0.8 V versus Ag/AgCl associated with the one-electron oxidation of **1** to $\mathbf{1}^{+\bullet}$. At a pH of **1**, a reductive peak was detected when the scan direction was reversed with the separation between the E_p^{ox} and E_p^{red} values equal to 70 mV, which is similar to the value observed under diffusion-controlled solution phase conditions (Figure 1). The general mechanism for the oxidation of **1** adhered to an electrode surface involves incorporation of the supporting electrolyte anion (X^-) into the solid material according to eq 2

$$1_{(solid)} + X^-_{(solution)} \rightleftharpoons [1^{+\bullet}][X^-]_{(solid)} + e^- \qquad (2)$$

The close similarity between the voltammetry of the solution phase compound (Figure 1) and that of the solid compound

TABLE 1: A Selection of Bond Lengths from Theoretical (EDF2/6-31+G*) Calculations[a,b]

	bond length/Å				
bond	$(CH_3)\alpha$-TOH[c,e]	**1**	$(CH_3)\alpha$-TOH$^{+\bullet}$[d]	$\mathbf{1}^{+\bullet}$	$(CH_3)\alpha$-TO^{+}[c,e]
C_1-C_2	1.404 *1.4055(14)*	1.405	1.437	1.438	1.454 *1.455(4)*
C_2-C_3	1.398 *1.3954(14)*	1.398	1.378	1.377	1.360 *1.355(4)*
C_3-C_4	1.399 *1.3974(15)*	1.405	1.424	1.438	1.498 *1.488(4)*
C_4-C_5	1.397 *1.3929(15)*	1.396	1.429	1.426	1.501 *1.491(4)*
C_5-C_6	1.406 *1.4012(15)*	1.407	1.378	1.381	1.359 *1.355(4)*
C_6-C_1	1.400 *1.3934(14)*	1.396	1.435	1.426	1.447 *1.447(4)*
C_6-C_7	1.511 *1.5132(14)*	1.508	1.506	1.503	1.504 *1.505(4)*
C_7-C_8	1.526 *1.5202(16)*	1.527	1.526	1.525	1.525 *1.518(4)*
C_8-C_9	1.526 *1.5217(16)*	1.528	1.519	1.521	1.519 *1.515(4)*
C_9-C_{13}	1.521 *1.5159(16)*	1.521	1.518	1.518	1.516 *1.518(5)*
C_9-C_{14}	1.529 *1.5207(16)*	1.529	1.524	1.524	1.521 *1.511(5)*
C_2-C_{10}	1.504 *1.5084(14)*	1.503	1.487	1.499	1.498 *1.499(4)*
C_3-C_{11}	1.508 *1.5113(15)*	1.503	1.498	1.499	1.490 *1.493(4)*
C_5-C_{12}	1.508 *1.5097(15)*	1.508	1.502	1.503	1.487 *1.495(4)*
C_4-O_1	1.377 *1.3950(13)*	1.374	1.329	1.318	1.217 *1.214(3)*
C_1-O_2	1.374 *1.3827(12)*	1.374	1.314	1.318	1.289 *1.282(3)*
C_9-O_2	1.440 *1.4566(12)*	1.441	1.487	1.483	1.510 *1.520(4)*

[a] Results from X-ray crystallographic measurements are in italics. [b] Atomic numbering system is given in Scheme 3. [c] Values from reference 5c. [d] Values from reference 5d. [e] Values from reference 5e.

SCHEME 3: Atomic Numbering System for the Theoretical Values Given in Table 1[a]

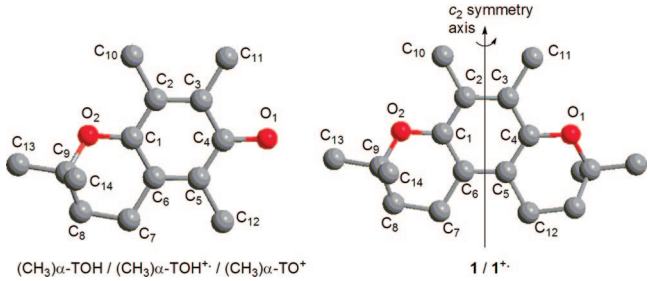

[a] Hydrogen atoms are omitted for clarity.

SCHEME 4: Quinoid Structure of $\mathbf{1}^{+\bullet}$

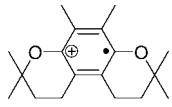

(Figure 5) indicates that the coupled electron and ion transport within the adhered compound are rate determining.[16] Therefore, the supporting electrolyte anion is readily able to diffuse into and out of the solid material during the potential cycling experiments.

At pH 1, the first scan often showed a higher current response after the oxidation process than the second and subsequent scans, which is likely to be due to an alteration of the electroactive material on the electrode surface during the first scan. The solid material can exist attached to the electrode in a number of forms (thin films, thick films, microcrystalline particles or as a combination of morphologies) and an applied potential can alter the structure of the solid.[16b] By measuring the charge passed during the first and subsequent scans and knowing the amount of solid material adhered to the electrode, it was possible to calculate that amount of material that was oxidized during any one scan. It was estimated that only around 1−2% of material underwent oxidation during a CV experiment.

At all pH values, apart from the first scan, the second and subsequent scans always showed a diminishing peak current with repetitive cycling, caused by material being lost (dissolving) from the electrode with each scan. It is likely that $\mathbf{1}^{+\bullet}$ is at least partly soluble in water; therefore with each cycle a percentage is removed from the electrode surface. A further feature of the voltammograms that supports some material being removed from the electrode surface with repetitive cycling is that within any one cycle the peak current for the reverse scan is always smaller than the forward scan. Furthermore, at faster scan rates (50 V s^{-1}) the diminishing current observed with repetitive cycling was less than at slower scan rates, due to less material being lost because less time was available for dissolution. The ΔE_{pp} values obtained at 50 V s^{-1} were greater than those obtained at slower scan rates but quite similar to the ΔE_{pp} values obtained at an equivalent scan rate when the experiments were performed with the compound dissolved in CH_3CN. Therefore, the increasing ΔE_{pp} values with increasing scan rate are likely to be caused by the effects of uncompensated solution resistance, rather than slow heterogeneous electron or ion transfer.

At a scan rate of 0.1 V s^{-1}, the voltammograms became progressively less chemically reversible as the pH was increased (Figure 5), so that at pH 13 only a forward oxidation process was observed and a relatively large decrease in current was seen between the first and second scans. The reason for the decrease in current could be two-fold. In one instance, the increase in pH could favor the dissolution of the positively charged solid compound. This is supported by the experiments at faster scan rates which show that the chemical reversibility begins to return (Figure 5), although there is still a large decrease in current between cycles, suggesting that dissolution is a major process. The alternative mechanism could be if the cationic compound were more reactive at high pH and underwent a hydrolysis type reaction to form a hydroxylated compound. The exact identity of the supporting electrolyte anion (other than hydroxide) is not considered to be critical to the chemical reversibility, since the change observed in the reversibility of the voltammograms at pH values of 1, 3, 5, 7, 9, 11, and 13 were systematic, despite different buffers used at pH 1, pH 3−7, and pH 9−13 (see Experimental Section).

3.6. Computational Section. High level ab initio calculations were performed on **1** and $\mathbf{1}^{+\bullet}$ in order to determine the structure of the cation radical and to calculate the infrared spectrum. The results were compared with the theoretical results already reported for the cationic forms of the α-tocopherol model compound, $(CH_3)\alpha$-TOH, with the values summarized in Table 1 (and Scheme 3). Previously it was found that the structures

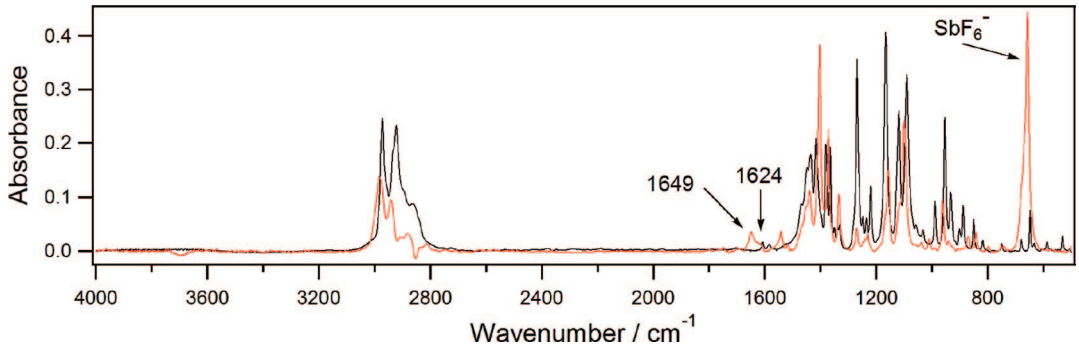

Figure 6. FTIR spectra of (black line) **1** and (red line) $\mathbf{1}^{+\bullet}(\mathbf{SbF_6^-})$ obtained by oxidizing **1** with 1 mol equivalent of $NOSbF_6$.

(bond lengths and bond angles) predicted by theoretical calculations were very close to the structural data obtained by X-ray crystallographic studies,[5e] and it is therefore reasonable to expect that the theoretical values for **1** and $\mathbf{1}^{+\bullet}$ are accurate. For ease of comparison, the same atomic numbering system was used for the vitamin E model compounds as for $\mathbf{1/1}^{+\bullet}$ (Scheme 3) even though the higher symmetry of $\mathbf{1/1}^{+\bullet}$ clearly made some bond lengths coincident.

The results in Table 1 illustrate that the analogous calculated bond lengths for $(CH_3)\alpha$-TOH and compound **1** were very close (in most instances within 0.005 Å). Furthermore, the comparable calculated bond lengths for the one-electron oxidized compounds [$(CH_3)\alpha$-$TOH^{+\bullet}$ and $\mathbf{1}^{+\bullet}$] were also very close indicating that the structure and positive charge distribution within $\mathbf{1}^{+\bullet}$ is similar to $(CH_3)\alpha$-$TOH^{+\bullet}$. Both $\mathbf{1}^{+\bullet}$ and $(CH_3)\alpha$-$TOH^{+\bullet}$ undergo a shortening of the C_2-C_3 and C_5-C_6 bonds compared to the uncharged starting material, indicating that the charged compounds begin to take on the structure expected for a quinoid type compound (Scheme 4). The results in Table 1 indicate that the structure of the phenoxonium cation [$(CH_3)\alpha$-TO^+] is even closer to that expected for a quinone with relatively short C_2-C_3 and C_5-C_6 (double) bonds and elongated C_1-C_2, C_3-C_4, C_5-C_6 and C_6-C_1 (single) bonds compared to the neutral starting material.

3.7. IR Spectroscopy. The infrared spectra of **1** (black line) and $\mathbf{1}^{+\bullet}(SbF_6^-)$ (red line) prepared by one-electron chemical oxidation of **1** with $NOSbF_6$ are given in Figure 6. The IR spectrum of **1** is very similar to $\mathbf{1}^{+\bullet}$ showing a number of absorbances at identical wavenumbers. However, notable differences in the IR spectrum of $\mathbf{1}^{+\bullet}$ (SbF_6^-) compared to **1** are the appearance of relatively weak absorbances at 1624 and 1649 cm^{-1}, which are associated with the "asymmetric and symmetric ring stretching modes" respectively, that result as the cation radical approaches a quinoid structure (Scheme 4). The symmetric ring stretching mode originates from the C_2-C_3 and C_5-C_6 (Scheme 3) bonds symmetrically stretching and contracting, while the carbon−oxygen bonds simultaneously stretch and contract. The asymmetric ring stretching mode is associated with the C_2-C_3 and C_5-C_6 bonds (Scheme 3) contracting and stretching not in unison (coupled with other atoms undergoing bond stretching and contraction). The theoretical calculations predicted the asymmetric and symmetric ring stretching modes at 1638 and 1696 cm^{-1}, respectively, which is up to 50 cm^{-1} higher than that observed experimentally, but of a similar level of accuracy previously found for the infrared vibrations of the phenoxonium cation.[5c]

These asymmetric and symmetric ring stretching modes were not previously detected in the infrared spectrum of $(CH_3)\alpha$-$TOH^{+\bullet}$,[5d] but this is likely to be because of their relatively weak intensity and because of the difficulty in handling solutions of $(CH_3)\alpha$-$TOH^{+\bullet}$ for infrared spectroscopic analysis [$(CH_3)\alpha$-$TOH^{+\bullet}$ has not to date been isolated as a solid compound].

4. Discussion

This work has demonstrated that compounds **1**−**3** can be oxidized to their respective radical cations in simple one-electron chemically reversible electron transfer processes, either heterogeneously at solid electrodes or homogeneously using NO^+ as the oxidant. Other chemical oxidants should also generate the radical cations providing that their oxidation potentials are $> +0.5$ V versus Fc/Fc^+. Compound **1** contains a fully methylated aromatic ring and is hence the most closely related to α-TOH. The reduction potential of $\mathbf{1}^{+\bullet}$ and its spectroscopic and structural properties are very similar to those of α-$TOH^{+\bullet}$. However, the lifetime of $\mathbf{1}^{+\bullet}$ is considerably longer than the lifetime of α-$TOH^{+\bullet}$ in aqueous and nonaqueous solvents because it contains an aprotic cyclic ether linkage in place of a hydroxyl group and because the methyl groups in the aromatic ring provide steric hindrance from coupling reactions to other cation radicals (as occurs for the less methyl substituted $\mathbf{2}^{+\bullet}$ and $\mathbf{3}^{+\bullet}$). Therefore, it can be concluded that $\mathbf{1}^{+\bullet}$ is a good "model" compound for examining the reductive properties of α-$TOH^{+\bullet}$.

It is generally thought that the biological antioxidant function of vitamin E occurs via a hydrogen atom transfer (HAT) mechanism where a reactive free radical ($R^\bullet$) reacts with the phenolic hydrogen atom (eq 3)[1]

$$R^\bullet + \alpha\text{-TOH} \rightleftharpoons RH + \alpha\text{-}TO^\bullet \quad (3)$$

Detailed kinetic experiments have demonstrated that the HAT mechanism involves strong interactions with the solvent molecules.[1d] In theory, it is possible that the reactive free radicals can also react with vitamin E through electron transfer (ET) and proton transfer (PT) reactions, which would lead to the radical cation (α-$TOH^{+\bullet}$) (eq 4) and phenoxyl radical (α-$TO^\bullet$) (eq 5) intermediates

$$R^\bullet + \alpha\text{-TOH} \rightleftharpoons R^- + \alpha\text{-}TOH^{+\bullet} \quad (4)$$

$$\alpha\text{-}TOH^{+\bullet} \rightleftharpoons \alpha\text{-}TO^\bullet + H^+ \quad (5)$$

Whether reaction 3 or reaction 4 occurs depends on the oxidizing ability of the $R^\bullet$ group. The role of α-$TOH^{+\bullet}$ in the antioxidant chemistry of vitamin E has not been ascertained,[1] although it is logical that under certain conditions reaction 4 should occur if the free radical is a strong enough oxidant. It has been proposed that α-$TOH^{+\bullet}$ is able to react with carotenoids (CAR) in a ET mechanism subsequently regenerating vitamin E and thereby giving the carotenoids synergistic antioxidant properties (eq 6)[17]

$$\alpha\text{-}TOH^{+\bullet} + CAR \rightleftharpoons \alpha\text{-TOH} + CAR^{+\bullet} \quad (6)$$

Electron paramagnetic resonance (EPR) experiments have shown that α-$TO^\bullet$ does not undergo an ET reaction to produce the carotenoid cation radicals,[18] most likely because it is not a

powerful enough oxidant (α-TO$^{\bullet}$ is reduced at approximately +0.15 V versus Fc/Fc^{+} in CH_3CN compared to +0.5 V versus Fc/Fc^{+} for α-TOH$^{+\bullet}$).[5h] A major difficulty in studying reaction 6 is that the cation radical of vitamin E is very acidic and not so long-lived (except in organic solvents containing strong acids[4,5] or in CH_2Cl_2 at low temperatures[19]), therefore, the phenoxyl radical will immediately form (eq 5). Thus, **1**$^{+\bullet}$ is potentially useful as a model compound to determine the oxidizing efficiency of α-tocopherol under homogeneous oxidizing conditions, especially in low dielectric constant solvents where the formal reduction potentials are difficult to determine experimentally. The replacement of one of the methyl groups at the quaternary carbons (C_{13} or C_{14} in Scheme 3) with a "phytyl chain" ($C_{16}H_{33}$) would give a lipid soluble species suitable for in vivo or in vitro studies. Previously, it was found that the phytyl chain in the natural compound is unimportant to the electrochemical properties of α-TOH and is unlikely to affect the lifetime of **1**$^{+\bullet}$ (or oxidation potential of **1**).

In conclusion, compound **1**$^{+\bullet}$ is a suitable long-lived model for testing the oxidizing abilities of the radical cation of vitamin E (α-TOH$^{+\bullet}$) under homogeneous conditions, without the additional complication of a deprotonation reaction. Electrochemical and spectroscopic experiments combined with theoretical calculations, indicate that the formal reduction potential, the structure, and the charge distribution of **1**$^{+\bullet}$ are similar to α-TOH$^{+\bullet}$, despite the absence of a hydroxyl group.

Acknowledgment. This work was supported by a Nanyang Technological University research Grant (SUG42/06).

Supporting Information Available: ^{1}H and ^{13}C NMR spectra from synthetic experiments and results from theoretical molecular orbital calculations. This material is available free of charge via the Internet at http://pubs.acs.org.

References and Notes

(1) (a) Traber, M. G.; Atkinson, J. *Free Rad. Bio. Med.* **2007**, *43*, 4–15. (b) Burton, G. W.; Ingold, K. U. *Acc. Chem. Res.* **1986**, *19*, 194–201. (c) Bowry, V. W.; Ingold, K. U. *Acc. Chem. Res.* **1999**, *32*, 27–34. (d) Litwinienko, G.; Ingold, K. U. *Acc. Chem. Res.* **2007**, *40*, 222–230.

(2) (a) Tasinato, A.; Boscoboinik, D.; Bartoli, G.-M.; Maroni, P.; Azzi, A. *Proc. Natl. Acad. Sci. U.S.A.* **1995**, *92*, 12190–12194. (b) Azzi, A.; Stocker, A. *Prog. Lipid Res.* **2000**, *39*, 231–255. (c) Ricciarelli, R.; Zingg, J.-M.; Azzi, A. *Biol. Chem.* **2002**, *383*, 457–465. (d) Azzi, A.; Ricciarelli, R.; Zingg, J.-M. *FEBS Lett.* **2002**, *519*, 8–10. (e) Melton, L. *New Sci.* **2006**, *191*, 40–43. (f) Azzi, A. *Free Radical Biol. Med.* **2007**, *43*, 16–21. (g) Azzi, A. *Biochem. Biophys. Res. Commun.* **2007**, *362*, 230–232.

(3) (a) Speiser, B.; Rieker, A. *J. Chem. Res. (S)* **1977**, 314–315. (b) Speiser, B.; Rieker, A. *J. Electroanal. Chem.* **1979**, *102*, 373–395. (c) Speiser, B.; Rieker, A. *J. Electroanal. Chem.* **1980**, *110*, 231–246. (d) Hammerich, O.; Svensmark, B. In *Organic Electrochemistry*, 3rd ed.; Lund, H., Baizer, M. M., Eds.; Marcel Dekker: New York, 1991; Chapter 16. (e) Rieker, A.; Beisswenger, R.; Regier, K. *Tetrahedron* **1991**, *47*, 645–654. (f) Eickhoff, H.; Jung, G.; Rieker, A. *Tetrahedron* **2001**, *57*, 353–364.

(4) (a) Parker, V. D. *J. Am. Chem. Soc.* **1969**, *91*, 5380–5381. (b) Svanholm, U.; Bechgaard, K.; Parker, V. D. *J. Am. Chem. Soc.* **1974**, *96*, 2409–2413.

(5) (a) Webster, R. D. *Electrochem. Commun.* **1999**, *1*, 581–584. (b) Williams, L. L.; Webster, R. D. *J. Am. Chem. Soc.* **2004**, *126*, 12441–12450. (c) Lee, S. B.; Lin, C. Y.; Gill, P. M. W.; Webster, R. D. *J. Org. Chem.* **2005**, *70*, 10466–10473. (d) Wilson, G. J.; Lin, C. Y.; Webster, R. D. *J. Phys. Chem. B* **2006**, *110*, 11540–11548. (e) Lee, S. B.; Willis, A. C.; Webster, R. D. *J. Am. Chem. Soc.* **2006**, *128*, 9332–9333. (f) Webster, R. D. *Acc. Chem. Res.* **2007**, *40*, 251–257. (g) Peng, H. M.; Webster, R. D. *J. Org. Chem.* **2008**, *73*, 2169–2175. (h) Yao, W. W.; Peng, H. M.; Webster, R. D. *J. Phys. Chem. B* **2008**, *112*, 6847–6855.

(6) Nanni, E. J., Jr.; Stallings, M. D.; Sawyer, D. T. *J. Am. Chem. Soc.* **1980**, *102*, 4481–4485.

(7) Fry, A. J.; Britton, W. E. In *Laboratory Techniques in Electroanalytical Chemistry*; Kissinger, P. T., Heineman, W. R., Eds.; Marcel Dekker: New York, 1984; Chapter 13.

(8) (a) Dean, F. M.; France, S. N.; Oyman, U. *Tetrahedron.* **1988**, *44*, 4857–4862. (b) Patel, A.; Liebner, F.; Netscher, T.; Mereiter, K.; Rosenau, T. *J. Org. Chem.* **2007**, *72*, 6504–6512.

(9) Webster, R. D.; Bond, A. M.; Schmidt, T. *J. Chem. Soc., Perkin Trans. 2* **1995**, 1365–1374.

(10) (a) Webster, R. D.; Heath, G. A.; Bond, A. M. *J. Chem. Soc., Dalton Trans.* **2001**, 3189–3195. (b) Webster, R. D.; Heath, G. A. *Phys. Chem. Chem. Phys.* **2001**, *3*, 2588–2594.

(11) Shao, Y.; Fusti Molnar, L.; Jung, Y.; Kussmann, J.; Ochsenfeld, C.; Brown, S. T.; Gilbert, A. T. B.; Slipchenko, L. V.; Levchenko, S. V.; O'Neill, D. P., Jr.; Lochan, R. C.; Wang, T.; Beran, G. J. O.; Besley, N. A.; Herbert, J. M.; Lin, C. Y.; Van Voorhis, T.; Chien, S. H.; Sodt, A.; Steele, R. P.; Rassolov, V. A.; Maslen, P. E.; Korambath, P. P.; Adamson, R. D.; Austin, B.; Baker, J.; Byrd, E. F. C.; Dachsel, H.; Doerksen, R. J.; Dreuw, A.; Dunietz, B. D.; Dutoi, A. D.; Furlani, T. R.; Gwaltney, S. R.; Heyden, A.; Hirata, S.; Hsu, C.-P.; Kedziora, G.; Khalliulin, R. Z.; Klunzinger, P.; Lee, A. M.; Lee, M. S.; Liang, W.; Lotan, I.; Nair, N.; Peters, B.; Proynov, E. I.; Pieniazek, P. A.; Rhee, Y. M.; Ritchie, J.; Rosta, E.; Sherrill, C. D.; Simmonett, A. C.; Subotnik, J. E.; Woodcock, H. L., III; Zhang, W.; Bell, A. T.; Chakraborty, A. K.; Chipman, D. M.; Keil, F. J.; Warshel, A.; Hehre, W. J.; Schaefer, H. F., III; Kong, J.; Krylov, A. I.; Gill, P. M. W.; Head-Gordon, M. *Phys. Chem. Chem. Phys.* **2006**, *8*, 3172–3191.

(12) *Spartan 04* for Macintosh; Wavefunction Inc.: Irvine, CA. 2004.

(13) Lin, C. Y.; George, M. W.; Gill, P. M. W. *Aust. J. Chem.* **2004**, *57*, 365–370.

(14) Gill, P. M. W.; Johnson, B. G.; Pople, J. A. *Chem. Phys. Lett.* **1993**, *209*, 506–512.

(15) (a) Rudolph, M. *J. Electroanal. Chem.* **2003**, *543*, 23–29. (b) Rudolph, M. *J. Electroanal. Chem.* **2004**, *571*, 289–307. (c) Rudolph, M. *J. Electroanal. Chem.* **2003**, *558*, 171–176. (d) Rudolph, M. *J. Comput. Chem.* **2005**, *26*, 619–632. (e) Rudolph, M. *J. Comput. Chem.* **2005**, *26*, 633–641. (f) Rudolph, M. *J. Comput. Chem.* **2005**, *26*, 1193–1204.

(16) (a) Marken, F.; Webster, R. D.; Bull, S. D.; Davies, S. G. *J. Electroanal. Chem.* **1997**, *437* (1−2), 209–218. (b) Bond, A. M. In *Broadening Electrochemical Horizons*; Oxford University Press: Oxford, 2002; Chapter 5. (c) Banks, C. E.; Davies, T. J.; Evans, R. G.; Hignett, G.; Wain, A. J.; Lawrence, N. S.; Wadhawan, J. D.; Marken, F.; Compton, R. G. *Phys. Chem. Chem. Phys.* **2003**, *5*, 4053–4069.

(17) Edge, R.; Land, E. J.; McGarvey, D.; Mulroy, L.; Truscott, T. G. *J. Am. Chem. Soc.* **1998**, *120*, 4087–4090.

(18) Valgimigli, L.; Lucarini, M.; Pedulli, G. F.; Ingold, K. U. *J. Am. Chem. Soc.* **1997**, *119*, 8095–8096.

(19) Lehtovuori, P.; Joela, H. *Phys. Chem. Chem. Phys.* **2002**, *4*, 1928–1933.

JP804135E